Heliyon 10 (2024) e27959

Contents lists available at ScienceDirect

Heliyon

journal homepage: www.cell.com/heliyon

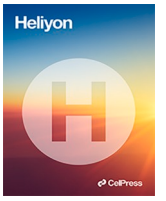

Research article

AURKA promotes renal cell carcinoma progression via regulation of CCNB1 transcription

Jiling Wen [a], Xuechun Wang [b], Guosheng Yang [a], Junhua Zheng [c,*]

[a] Department of Urology, Shanghai East Hospital, Tongji University School of Medicine, No.150, Jimo Road, Shanghai, 200120, China
[b] Department of Biological Sciences, University of Notre Dame, Notre Dame, 46556, IN, USA
[c] Department of Urology, Renji Hospital, School of Medicine, Shanghai Jiao Tong University, No.160, Pujian Road, Shanghai, 200127, China

ARTICLE INFO

Keywords:
AURKA
RCC
Transcriptional regulation
CCNB1
Proliferation

ABSTRACT

AURKA is a member of the serine/threonine kinase family and its kinase activity is crucial for the progression of mitosis. Recent studies have highlighted the therapeutic significance of AURKA inhibition in multiple cancer types. However, the specific mechanisms by which AURKA contributes to the progression of renal cell carcinoma (RCC) have not been fully elucidated. In this study, AURKA expression level was identified in human RCC tissues by immunohistochemical (IHC) staining. The function of AURKA on cell malignant phenotypes was evaluated *in vitro* after AURKA inhibition. The subcutaneous xenograft was conducted to confirm the *in vivo* effect of AURKA knockdown on growth of RCC cells. Finally, Co-IP, luciferase assay and ChIP experiments were performed to reveal the regulatory mechanism of AURKA on CCNB1. Our results showed a significant upregulation of AURKA in RCC tissues and cell lines, and a high AURKA expression was associated with poor prognosis. AURKA knockdown inhibited RCC cell proliferation and migration, induced cell apoptosis, and led to G1/G2 phase arrest. This effect was further confirmed by the use of an AURKA inhibitor. Mechanistically, AURKA interacted with E2F1, and subsequently recruited it to the promoter region of CCNB1. CCNB1 expression was essential for AURKA-induced RCC progression. Collectively, our results suggested that AURKA plays an important role in development of RCC via regulating CCNB1 transcription.

1. Introduction

Cancer is an important problem in global public health and one of the main causes of human death. Effective control of cancer is a crucial way to improve average life expectancy [1,2]. Renal cell carcinoma (RCC) is a type of malignant tumor arising from the urothelial system of the renal parenchyma, accounting for more than 90% of all malignant tumors of the kidney [2]. According to recent statistics, RCC ranks sixth and ninth among the most common malignancies in men and women in the United States, respectively [1]. Clear cell renal cell carcinoma (ccRCC) is the most common pathological type of RCC, accounting for approximately 80–85% of all types of RCC [3,4]. Although RCC is classified as a low-grade malignant tumor, the treatment of RCC remains challenging due to the solid organ nature and strong compensatory function of the kidney. Additionally, RCC typically manifests insidiously, resulting in about 30% of patients having advanced-stage disease or distant metastasis at the time of diagnosis, thereby causing great difficulties in treatment [3]. At present, surgery is still the first choice for the treatment of early RCC, but it is difficult to eradicate the tumor and

* Corresponding author.
E-mail address: zhengjh0471@sina.com (J. Zheng).

https://doi.org/10.1016/j.heliyon.2024.e27959
Received 23 January 2024; Received in revised form 5 March 2024; Accepted 8 March 2024
Available online 3 April 2024

prone to postoperative recurrence or metastasis. Common chemotherapeutic drugs also fail to eradicate tumor cells and have strong toxic side effects [5,6]. Therefore, there is still a lack of effective treatment strategies for RCC. In recent years, targeted therapy has emerged as a promising approach for treating RCC. To date, 9 targeted drugs, such as sunitinib and sorafenib, have been approved by the US Food and Drug Administration for the clinical treatment of RCC [7,8]. Therefore, it is particularly important to explore more novel biomarkers of RCC and develop more effective targets as well as corresponding treatments for improving prognosis of ccRCC patients.

AURKA (also known as Aurora-A) is a member of the serine/threonine kinase family whose kinase activity is essential for mitotic progression. In late S/early G2 phase of the cell cycle, AURKA binds to the centrosome, where it recruits centrally important components of the central canal, including γ-tubulin, to the centrosome and then contributes to driving centrosome maturation [9,10]. AURKA, assisted by Bora, mediates the activation of the mitotic kinase polo-like kinase (PLK1) by phosphorylation to achieve G2/M phase transition of the cell cycle [11]. Therefore, the AURKA/PLK1 signaling network plays an important role throughout mitosis. In recent years, the regulatory role of AURKA in tumors has aroused great interest from researchers [12]. Normally, AURKA plays its role only in G2/M phase of mitosis. In tumor cells, AURKA is expressed throughout the cycle of cell division, affecting the function of other proteins in the cytoplasm, such as inhibiting the activity of tumor suppressor proteins such as p53 and BRCA1, leading to the development of tumors [12–15]. Therefore, in recent years, the in-depth study of the downstream mechanism by which AURKA regulates tumor cell phenotype, as well as the development of small molecule kinase inhibitors targeting AURKA, has become the focus of research in the field of AURKA-related research.

In this study, we determined the expression of AURKA in RCC tissues and its correlation with overall survival and other clinical histopathological features. The loss-of-function experiments of AURKA were then performed to investigate the effect of AURKA expression on malignant phenotypes of RCC cells. Furthermore, we identified that CCNB1 is the downstream target responsible for the modulation of AURKA oncogenic function in RCC. Specifically, we found that AURKA regulates CCNB1 expression through recruiting E2F1 to the promoter region of CCNB1. Taken together, our data provide a conceivable rationale for targeting the AURKA-CCNB1 axis in patients with RCC.

2. Materials and methods

2.1. Tissue microarray and immunohistochemical (IHC) analysis

The human microarray chip containing 147 human RCC tissues and 30 normal para-carcinoma tissues was used for determining expression of AURKA in RCC, and the according clinical pathological information was also collected. This study was approved by the Ethics Committee of Shanghai East Hospital, Tongji University (approval no. 2020-128). To perform immunohistochemical (IHC) staining of AURKA, the tissue slides underwent a series of preparation steps. First, the slides were dewaxed and rehydrated using xylene and different concentrations of alcohol. Subsequently, the slides were treated with 3% H2O2 and citrate buffer to repair the antigens. Next, anti-AURKA antibody (1:100; cat. no. ab52973; Abcam) was applied to the tissue slides and incubated overnight at 4 °C. After washing with phosphate-buffered saline (PBS), the sections were incubated with a secondary horseradish peroxidase (HRP)-conjugated goat anti-rabbit IgG antibody (1:400; cat. no. ab97080; Abcam) for 30 min at room temperature. The sections were then visualized using diaminobenzidine (DAB) chromogen and counterstained with hematoxylin. Following staining, the slides were dehydrated and mounted. Images of the stained slides were captured using a fluorescence microscope (Olympus Corporation). The stained slides were scored by two independent pathologists using the method proposed by Haonon et al. [16]. Briefly, the staining score was determined by multiplying the staining intensity and the percentage of positive tumor cells. The staining intensity was classified into four levels: no staining signal (0), light yellow (1), pale brown (2), or seal brown (3). Similarly, the percentage of positive tumor cells was divided into four levels: 0–24% (1), 25–49% (2), 50–74% (3), and 75–100% (4). The product of these scores was calculated as the immunoreactivity grading score, ranging from 0 to 12. The scores were then grouped as follows: 0 (low expression), 1–3 (weak expression), 4–7 (moderate expression), and 8–12 (strong expression).

2.2. Bioinformatics analysis

Differential expression of AURKA and CCNB1 genes in KICH, KIRC and KIRP was analyzed based on The Cancer Genome Atlas (TCGA) database (https://cancergenome.nih.gov/). The corresponding clinical features information was also download and analyzed. Pearson's correlation analysis was applied to assess the association between expression of AURKA and clinical features of patients.

2.3. Cell culture and Barasertib treatment

Human normal proximal tubule epithelial cell line (HK-2) and RCC cell lines (786-O, ACHN, A498 and SN12C) were purchased from the Cell Bank of the Chinese Scientific Academy (Shanghai, China). All the cells were cultured in Gibco® DMEM-H medium (Thermo Fisher Scientific, Inc.), supplemented with 10% Gibco® fetal bovine serum (FBS) and 1% penicillin/streptomycin (100 U/ml) (Thermo Fisher Scientific, Inc.). Cells were maintained in an incubator at 37 °C in an atmosphere containing 5% CO_2.

The AURKA kinase inhibitor, Barasertib (AZD1152), was purchased from Astra Zeneca Pharmaceuticals (Macclesfield, Cheshire, UK) and dissolved in dimethyl sulfoxide (DMSO). The cells were treated with Barasertib at 25 nM for 48 h.

2.4. RNA interference and overexpresion

For AURKA and CCNB1 knockdown, three shRNA sequences targeting the human AURKA and CCNB1 gene (named shAURKA/CCNB1-1/2/3) were designed and synthesized by Shanghai Yibeirui Biomedical Science and Technology Co., Ltd. The lentiviral vectors of shAURKA/CCNB1-1/2/3 were generated using the BR-V108 plasmid. Following this, a second-generation lentiviruses of shAURKA/CCNB1-1/2/3 (10 μg) were generated by co-transfecting with the packaging (7.5 μg pMD2.G and 5 μg pSPAX2; Qiagen China Co., Ltd.) plasmids into 293T cells (Procell Life Science&Technology Co.,Ltd.), followed by viral concentration and purification. Lentivirus inserted scramble sequences (named shCtrl) were used as the negative controls for shAURKA/CCNB1-1/2/3. Similarly, AURKA and E2F1 overexpressed lentivirus vectors were prepared using GL005 plasmid, and then co-transfected with lentivirus packaging vectors to produce corresponding overexpressed lentiviruses, and the empty vector (named control) acted as a negative control. The aforementioned target sequences of shRNAs and sequence of shCtrl mentioned are shown in Table S1.

The transfection of lentiviruses in RCC cell lines was achieved using Lipofectamine™ 3000 (Thermo Fisher Scientific, Inc.) at 37 °C for 48–72 h. After confirming successful transduction via GFP expression observed 72 h post-infection using fluorescence microscopy, cells displaying robust fluorescent efficiency and fusion were isolated through puromycin selection (2 μg/mL) following lentiviral transfection. Subsequently, individual cells were cloned to create uniform populations expressing the desired modifications. The most effective interference target, determined by qPCR analysis for subsequent experiments, underwent validation for knockdown or overexpression at both mRNA and protein levels to ensure dependable and reproducible results.

2.5. Reverse transcription-quantitative PCR (RT-qPCR) analysis

The cellular samples were subjected to total RNA extraction using TRIzol® reagent (Sigma Aldrich; Merck KGaA), following the provided instructions. The concentration of the isolated RNA was measured at 260 nm using a NanoDrop 1000 spectrophotometer (Thermo Fisher Scientific, Inc.). Subsequently, the cDNA template was synthesized using HiScript II Q Select RT SuperMix (Vazyme Biotech Co., Ltd.), following the manufacturer's protocol. For the real-time quantitative polymerase chain reaction (RT-qPCR), aliquots of 10 μl from the reverse transcription (RT) reactions were mixed with SYBR™ Green PCR Master Mix (Vazyme Biotech Co., Ltd.). The RT-qPCR reactions were carried out using a Biosystems 7500 Sequence Detection system. The internal control gene, GAPDH, was used for normalization purposes. Relative quantitative expression of targeted genes was calculated according to the $2^{-\Delta\Delta Cq}$ method, as previously described [17]. Sequences of the primers used for the PCR reactions are shown in Table S2.

2.6. Western blot (WB) analysis

Cellular samples were subjected to protein extraction using ice-cold radioimmunoprecipitation (RIPA) lysis buffer (Beyotime Institute of Biotechnology). The total protein content was determined using a BCA Protein Assay Kit (HyClone; Cytiva). Whole cell lysates were then fractionated by sodium dodecyl sulfate polyacrylamide gel electrophoresis (SDS-PAGE) using 10% gels (Invitrogen; Thermo Fisher Scientific, Inc.), with 10 μg of protein lysates loaded per lane for each sample. Subsequently, the separated proteins were transferred onto polyvinylidene difluoride (PVDF) membranes (MilliporeSigma). The membranes were then blocked with 5% nonfat skimmed milk at room temperature for 1 h and incubated overnight at 4 °C with primary antibodies listed in Table S3. Afterward, a secondary HRP-conjugated antibody, specifically goat anti-rabbit/mouse IgG, was added and allowed to incubate at room temperature for 2 h. The relative levels of the targeted proteins were visualized using enhanced chemiluminescence (ECL; MilliporeSigma). To quantify the Western blot results, ImageJ software (version 1.8.0; National Institutes of Health) was utilized. The signals were adjusted for background noise and normalized against the signal for GAPDH, which served as the internal control in these experiments.

2.7. Celigo cell counting assay

To assess cell proliferation, the celigo cell count assays were employed. In summary, 786-O and ACHN cells with stably knocked down AURKA were harvested and resuspended in complete medium. Subsequently, they were seeded into 96-well plates at a density of 1000 cells per well. The cells were then cultured continuously for 5 days, and each day the 96-well plates were scanned using the celigo system (Nexcelom). Finally, a cell proliferation curve was generated based on the collected cell count data.

2.8. Flow cytometric analysis

Flow cytometric analysis was employed to assess alterations in cell apoptosis and cycle distribution. To begin, 786-O and ACHN cells were infected with lentivirus or treated with Barasertib as indicated and seeded into 6-well plates at a density of 1×10^6 cells per well for 5 days. To evaluate cell apoptosis levels, the cells were harvested and treated with Annexin V (eBioscience; Thermo Fisher Scientific, Inc.) alone or Annexin V/Propidium Iodide (PI) staining simultaneously.

For analysis of cell cycle changes, the cells were collected, fixed with 4 °C pre-cooled 70% ethanol for 1 h, and stained with a mixture of PI and RNaseA (Takara Biotechnology Co., Ltd.). Subsequently, a flow cytometer (Millipore Guava easyCyte HT; MilliporeSigma) was utilized to measure the proportions of apoptotic cells and cells distributed among different stages of apoptosis. The data obtained were analyzed using GuavaSoft 3.0 software (Merck KGaA).

2.9. CCK-8 assay

786-O and ACHN cells were plated into 96-well plates at a density of 2×10^3 cells per well. After 24 h of cell seeding, the cells were treated with 25 nM Barasertib for a duration of 48 h. Following the 48-h treatment, 10 μL of CCK-8 solution was added to each well at indicated time points. The cells were then incubated for an additional 4 h after the addition of the CCK-8 solution. The optical density (OD) values at 450 nm were determined using a microplate reader (Thermo, USA).

2.10. Wound-healing assay

To assess the degree of cell migration, wound healing assays were conducted. In brief, 786-O and ACHN cells that had been stably depleted of AURKA were seeded into 96-well plates at a density of 5×10^4 cells per well when they reached 90% confluence. On the following day, the cells were starved by incubating them with medium containing 0.5% FBS for 24 h. Subsequently, a scratch was created at the bottom center of the 96-well plate using a scratch tester, and the cells were then maintained in medium supplemented with 0.5% FBS at 37 °C. The distances migrated by the cells at different time points (0 h and 8 h) were assessed using Cellomics (Thermo Fisher Scientific, Inc.). Migration rates were calculated based on the measured migratory distances.

2.11. Transwell assay

786-O and ACHN cells (5×10^4) that had been transfected with the lentivirus were subjected to a Transwell assay using a kit from Corning, Inc., following the manufacturer's instructions. After trypsinization, the cells were resuspended in 100 μl of FBS-free medium and added to the upper chamber of the Transwell system. The lower chamber was filled with 600 μl of medium containing 30% FBS, creating a gradient to induce cell migration from the upper to the lower chamber. Incubation at 37 °C was carried out for 24 h. Following this incubation period, non-migratory cells on the lower surface of the membrane were gently removed using a cotton tip, and the migratory cells were stained with Giemsa for 5 min at room temperature. Subsequently, the numbers of migratory cells were visualized and counted using a fluorescence microscope.

2.12. Co-immunoprecipitation (Co-IP)

The Co-IP experiments were conducted following a previously described protocol [18]. To summarize, ACHN cell lysates were prepared in RIPA buffer and quantified using a BCA kit (HyClone-Pierce, USA). A total of 1.0 mg of protein was incubated with anti-E2F1 antibody at 4 °C overnight, followed by incubation with 20 μL of agarose beads at 4 °C for 2 h. The protein-antibody-bead complexes were then separated through centrifugation at 2000*g* for 1 min, and subsequently, the pellets were lysed with IP lysate buffer at 100 °C for 5 min. The immunoprecipitated proteins were further analyzed by WB, as described previously. The antibodies used in these experiments are listed in Table S3.

2.13. Dual-luciferase reporter assay

A luciferase reporter assay was conducted following a standard protocol as previously described [19]. Initially, luciferase reporter plasmids were constructed by inserting wild-type or mutant fragments from the CCNB1 promoter region into the GL002 luciferase reporter vector (Promega Madison, USA), referred to as CCNB1-WT or CCNB1-MUT, respectively. ACHN cells (1×10^4 cells/well) with or without AURKA overexpression were seeded in triplicate in 24-well plates and allowed to culture for 24 h. Subsequently, the E2F1-overexpressing plasmids and luciferase reporter plasmids were co-transfected using Lipofectamine™ 3000 (Thermo Fisher Scientific, Inc.). After 48 h of transfection, luciferase and Renilla signals were determined using the Dual Luciferase Reporter Assay Kit (Promega, Cat. No. E1980) in accordance with the manufacturer's instructions.

2.14. Chromatin immunoprecipitation (ChIP) assay

The chromatin immunoprecipitation (ChIP) assay was conducted using the SimpleChIP® Enzymatic Chromatin IP Kit (Cat No, 9002S, CST, USA) as the manufacturer's instructions. Briefly, ACHN cells with or without AURKA overexpression were crosslinked with 37% formaldehyde, followed by lysis in SDS buffer and sonication to fragment the DNA. Subsequently, the sonicated chromatin was incubated overnight at 4 °C with anti-E2F1 antibody to immunoprecipitate the protein-DNA complexes. The protein-DNA complexes were then isolated and the purified DNA was dissolved in nuclease-free water. Quantitative PCR (qPCR) analysis using primers specific to the CCNB1 promoter region was carried out using SYBR Green I Master (Roche, USA). The enrichment percentage = 2% × 2 [CT (input sample) − CT (IP sample)]. Normal IgG and histone H3 were used as negative and positive controls, respectively. The primers used for amplifying the CCNB1 promoter region are listed in Table S2. The antibodies employed in this assay are listed in Table S3.

2.15. Establishment of the mice xenograft model

A total of 16 BALB/c nude mice (15–17 g; 6-weeks-old male mice) were purchased from GemPharmatech Co., Ltd. (Jiangsu, China) and housed in a controlled environment free from pathogens. The holding room was maintained at a temperature of 20∼26 °C with

Table 1
Expression patterns of AURKA in ccRCC tissues and normal tissues were revealed in immunohistochemistry analysis.

AURKA expression	Tumor tissue		Normal tissue	
	Cases	Percentage	Cases	Percentage
Low	72	49.0%	26	86.7%
High	75	51.0%	4	13.3%

$P < 0.001$.

Table 2
Relationship between AURKA expression and tumor characteristics in patients with ccRCC.

Features	No. of patients	AURKA expression		*P* value
		low	high	
All patients	147	72	75	
Age (years)				0.161
≤57	75	41	34	
>57	72	31	41	
Gender				0.982
Male	104	51	53	
Female	43	21	22	
Grade				0.006
I	1	0	1	Pearson correlation = 0.229 (P = 0.005)
II	105	60	45	
III	38	11	27	
IV	3	1	2	
T Infiltrate				0.007
T1	119	65	54	Pearson correlation = 0.223 (P = 0.007)
T2	17	3	14	
T3	11	4	7	
Tumor size				0.365
≤4 cm	74	39	35	
>4 cm	73	33	40	
lymphatic metastasis (N)				0.596
N0	144	71	73	
N1	2	0	2	
N2	1	1	0	
Expression of PDL1				0.156
≤1	79	43	36	
>1	68	29	39	
Stage				0.009
1	119	65	54	Pearson correlation = 0.217 (P = 0.008)
2	16	2	14	
3	11	4	7	
4	1	1	0	

humidity level of 30~70%, following a 12-h light/dark cycle. The mice were provided with standard laboratory food and had access to clean drinking water *ad libitum*. The animal facility was well-ventilated and all cages were kept clean and hygienic condition to ensure the animals' health and welfare. The mice were randomly divided into four groups, including the NC, AURKA, shCCNB1 and AURKA + shCCNB1 groups, with four mice in each group. Subsequently, corresponding cells were subcutaneously injected into the flank area of mice to stimulate tumorigenicity. The tumor sizes were regularly monitored and the tumor volume was calculated using the formula: $V = \pi/6 \times L \times W^2$, where W represents the width at the widest point, and L denotes the perpendicular width. The tumor grew until they reached a maximum diameter of approximately 1.2 cm. On day 25, the mice were euthanized by intraperitoneal injection of 0.3% sodium pentobarbital (200 mg/kg, 0.2 ml/10 g). The tumor tissues of each mice were then isolated and weighted. Histopathological staining of Ki-67 (1:300; cat. no. ab16667; Abcam) was performed on the tumor tissues following the same procedure as AURKA staining in human tissues mentioned earlier. This animal study was approved by the Institutional Animal Care and Use Committee of Shanghai East Hospital, Tongji University (approval no. 2020-128). Throughout the experiments, all possible measures were taken to minimize suffering of the mice.

2.16. Statistical analysis

The statistical analysis was conducted using SPSS 22.0 (IBM Corp.) and GraphPad Prism 8.04 software (Dotmatics). The presented

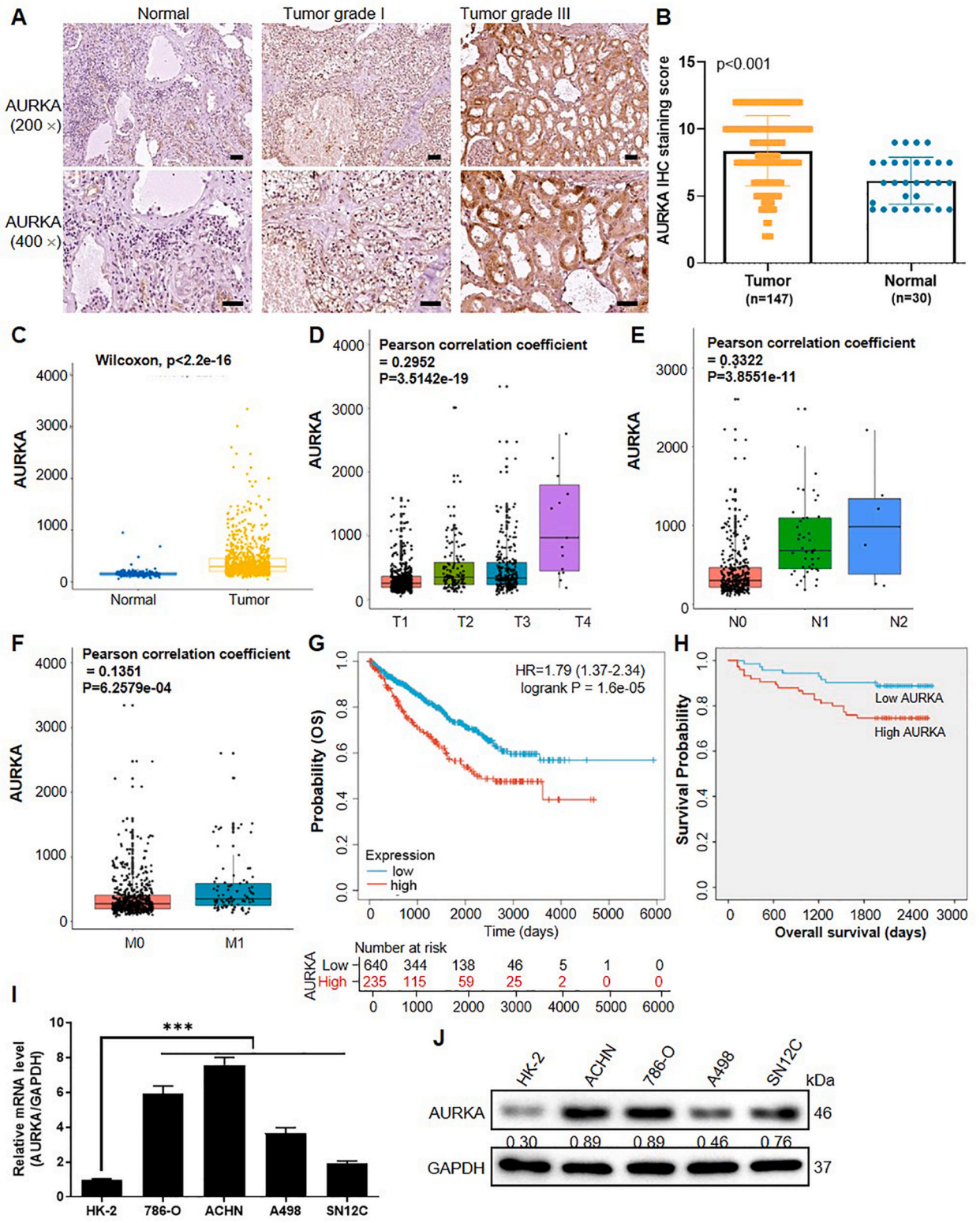

(caption on next page)

Fig. 1. Upregulation of AURKA in RCC is associated with poor prognosis. (A) IHC staining of AURKA in RCC tissues and normal para-carcinoma tissues of human tissues chip. n = 147 for patients with RCC, n = 30 for normal subjects. Scale bar represents 50 μm. (B) Score of AURKA staining in RCC and normal para-carcinoma tissues. (C–G) All analysis was performed based on the data from TCGA (KICH + KIRC + KIRP). n = 887 for patients with RCC (KICH + KIRC + KIRP), n = 128 for normal subjects. (C) Differential expression of AURKA in KICH, KIRC, and KIRP from TCGA. (D) Pearson correlation between AURKA expression and tumor T stage. (E) Pearson correlation between AURKA expression and tumor N stage. (F) Pearson correlation between AURKA expression and tumor M stage. (G) Kaplan-Meier analysis of correlation between AURKA expression and OS in TCGA and (H) human RCC tissues (n = 72 for RCC patients with low AURKA expression, n = 75 for RCC patients with high AURKA expression). (I) Relative mRNA and (J) protein levels of AURKA in human normal cell line (HK-2) and RCC cell lines (ACHN, 786-O, A498, SN12C). n = 3. ***$P < 0.001$. IHC, immunohistochemistry; TCGA, The Cancer Genome Atlas; KICH, kidney chromophobe; KIRC, kidney renal clear cell carcinoma; KIRP, kidney renal papillary cell carcinoma; OS, overall survival.

data are expressed as the mean ± standard deviation (SD). For comparisons between two groups, an unpaired two-tailed Student's t-test was employed. Multiple comparisons were assessed using ANOVA followed by a Tukey post-hoc test. Survival analysis was performed using Kaplan-Meier curves, and the log-rank test was used to determine statistical differences between two groups. The paired sign test and unpaired Mann-Whitney U analysis were used for statistical analysis of Tables 1 and 2, respectively. A significance level of $p < 0.05$ was considered statistically significant.

3. Results

3.1. Upregulation of AURKA in RCC is associated with poor prognosis

In preliminary stage of this study, a tissue microarray containing 147 tumor tissue samples and 30 normal ones was subjected to immunohistochemical (IHC) staining for estimating the correlation between AURKA and RCC. As shown in Table 1, statistical analysis, based on the grouping of high/low expression using IHC score median, indicated the significantly upregulated AURKA expression in tumor tissues in comparison with normal ones. The differential expression of AURKA could also be observed in the representative images shown in Fig. 1A, the quantitative results of AURKA IHC staining were shown in Fig. 1B. Data collected from TCGA (KICH + KIRC + KIRP) also revealed similar trend with our cohort (Fig. 1C). Moreover, the significantly positive correlation between AURKA expression with a series of tumor characteristics such as TNM level, pathological stage and tumor grade was displayed by the statistical analysis of TCGA data or results of tissue microarray (Fig. 1D–F and Table 2). Finally, survival analysis based on TCGA or our cohort indicated the significantly poorer overall survival (Fig. 1G-H) upon AURKA overexpression. Moreover, elevated expression levels of AURKA were further confirmed in RCC cell lines (Fig. 1I-J). Clearly, it was demonstrated that AURKA may be a key participator in the development of RCC.

3.2. In vitro loss-of-function assays reveal the tumor-inhibiting profile of AURKA inhibition

Lentiviruses packaging shRNA designed for silencing AURKA (shAURKA-1) as well as the negative control sequence (shCtrl) were prepared and used for constructing AURKA knockdown RCC cell lines 786-O and ACHN. The efficiency of AURKA knockdown was verified using qPCR and Western blot assays, which detected the mRNA and protein levels of AURKA, respectively (Fig. 2A-B). Subsequently, celigo cell counting assay indicated the significantly slower *in vitro* growth of 786-O and ACHN cells with AURKA knockdown (Fig. 2C). Correspondingly, the deficiency of AURKA also cause the increase of apoptotic cell percentage and the cell cycle arrest in G1 or G2 phase (Fig. 2D-E). Moreover, downregulation of anti-apoptotic and cell cycle progression-related proteins, such as Bcl-2, CCNB1, CCND1, and CCNA1, was observed following AURKA silencing. Conversely, the upregulation of the pro-apoptotic protein cleaved caspase-3 was evident (Fig. 2F-G). These findings provide compelling evidence affirming the role of AURKA in influencing both cell apoptosis and cell cycle progression. To further substantiate the promotional influence of AURKA on the malignant phenotypes of RCC cells, we employed Barasertib, an inhibitor of AURKA kinase. The results demonstrated that Barasertib treatment not only restrained cell proliferation but also prompted cell apoptosis (Fig. 2H-I), consistent with the functional outcomes observed with AURKA shRNA. On the other hand, both the scratch assay (Fig. 3A) and transwell assay (Fig. 3B) suggested that cell migration ability, the specific nature of cancer cells facilitating metastasis, was also weakened after knocking down AURKA. The Barasertib treatment showed a similar trend on cell migration ability in comparison with AURKA shRNA (Fig. 3C). Collectively, all results obtained from cell models are in accordance with our inference of the tumor-promoting role of AURKA in RCC development.

3.3. Overexpressed AURKA in ACHN cells regulates CCNB1 transcription

To identify AURKA-target genes involved in the RCC progression, we screened the co-expressed genes with AURKA using Coexpedia (https://www.coexpedia.org/). As shown in Fig. 4A, CCNB1 showed the highest likelihood scores, suggested that AURKA might promotes malignant phenotypes of RCC cells via CCNB1. Moreover, the correlation analysis of AURKA and CCNB1 in TCGA-KIRC indicated that the expression of AURKA was positively correlated with that of CCNB1, and there might be some regulatory mechanism between them ($p < 0.001$) (Fig. 4B). We next determined the overexpression of CCNB1 in TCGA (KICH + KIRC + KIRP) compared to normal control tissues (Supplementary F. 1A), and we found that high level of CCNB1 predicted an advanced tumor stage and TNM stage, as well as the short overall survival ($p < 0.001$) (Supplementary F. 1B–1F). Moreover, the RCC cell lines also showed an elevated expression levels of CCNB1 compared to the normal HK-2 cell (Fig. 4C-D). Notably, downregulation of AURKA significantly decreased

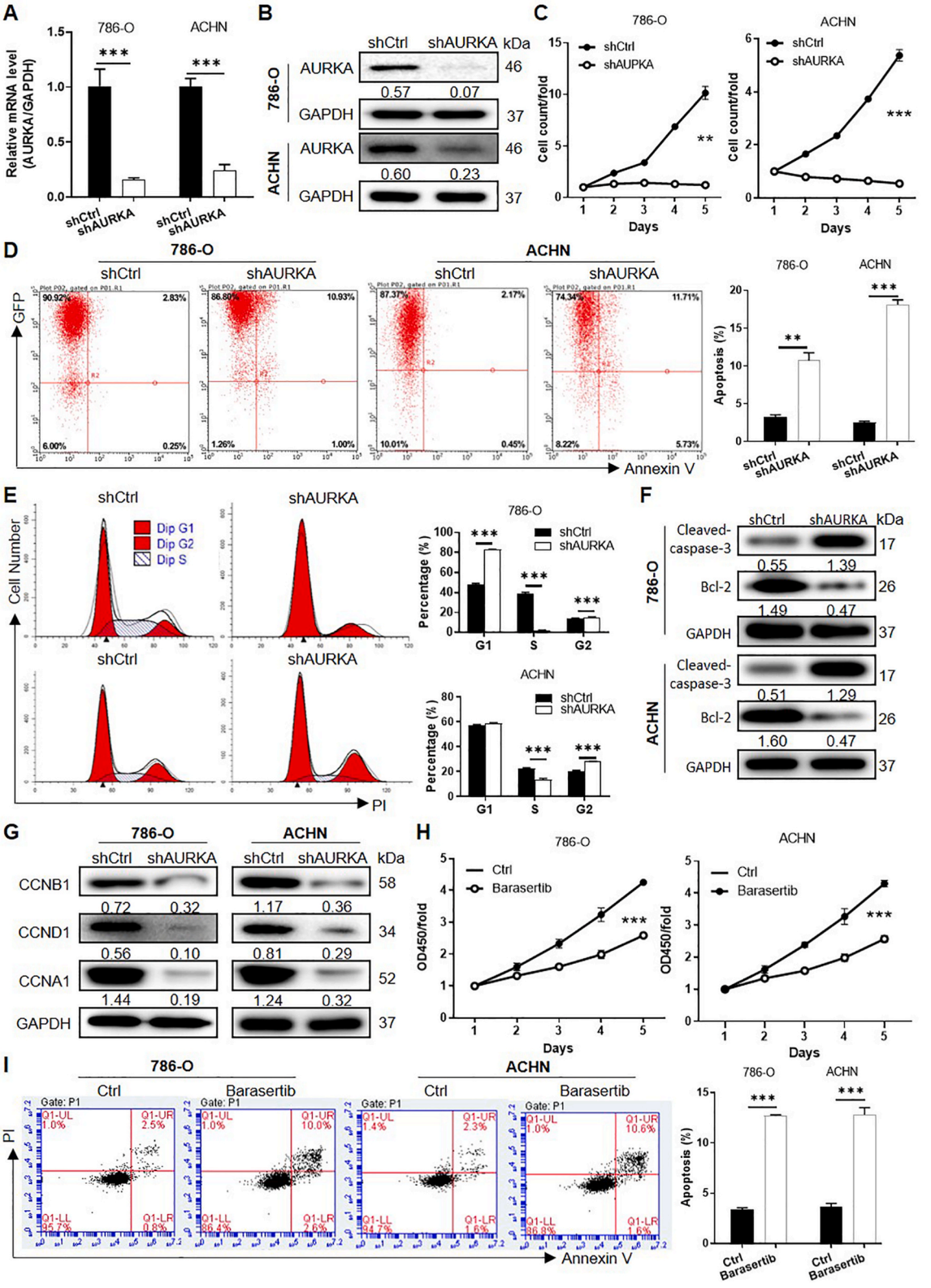

(caption on next page)

Fig. 2. *In vitro* loss-of-function assays reveal the tumor-inhibiting profile of AURKA inhibition. (A) AURKA knockdown efficiency was validated at mRNA and (B) protein levels. GAPDH served as an inner control. n = 3. (C) The effect of AURKA knockdown on cell proliferation in 786-O and ACHN cells was explored using Celigo cell count assay. n = 3. (D) The flow cytometry was employed for evaluating effects of AURKA knockdown on cell apoptosis and (E) cell cycle distribution. n = 3. (F–G) Western blot assays detected the indicated protein levels in 786-O and ACHN cells transfected with shCtrl or shAURKA lentivirus. n = 3. (H) The effect of AURKA inhibition, induced by AURKA inhibitor Barasertib, on cell proliferation in 786-O and ACHN cells was investigated through CCK-8 assay. n = 3. (I) The influence of Barasertib on cell apoptosis was determined by flow cytometry. The cells were treated with 25 nM Barasertib for 48 h n = 3. $^{**}P < 0.01$, $^{***}P < 0.001$.

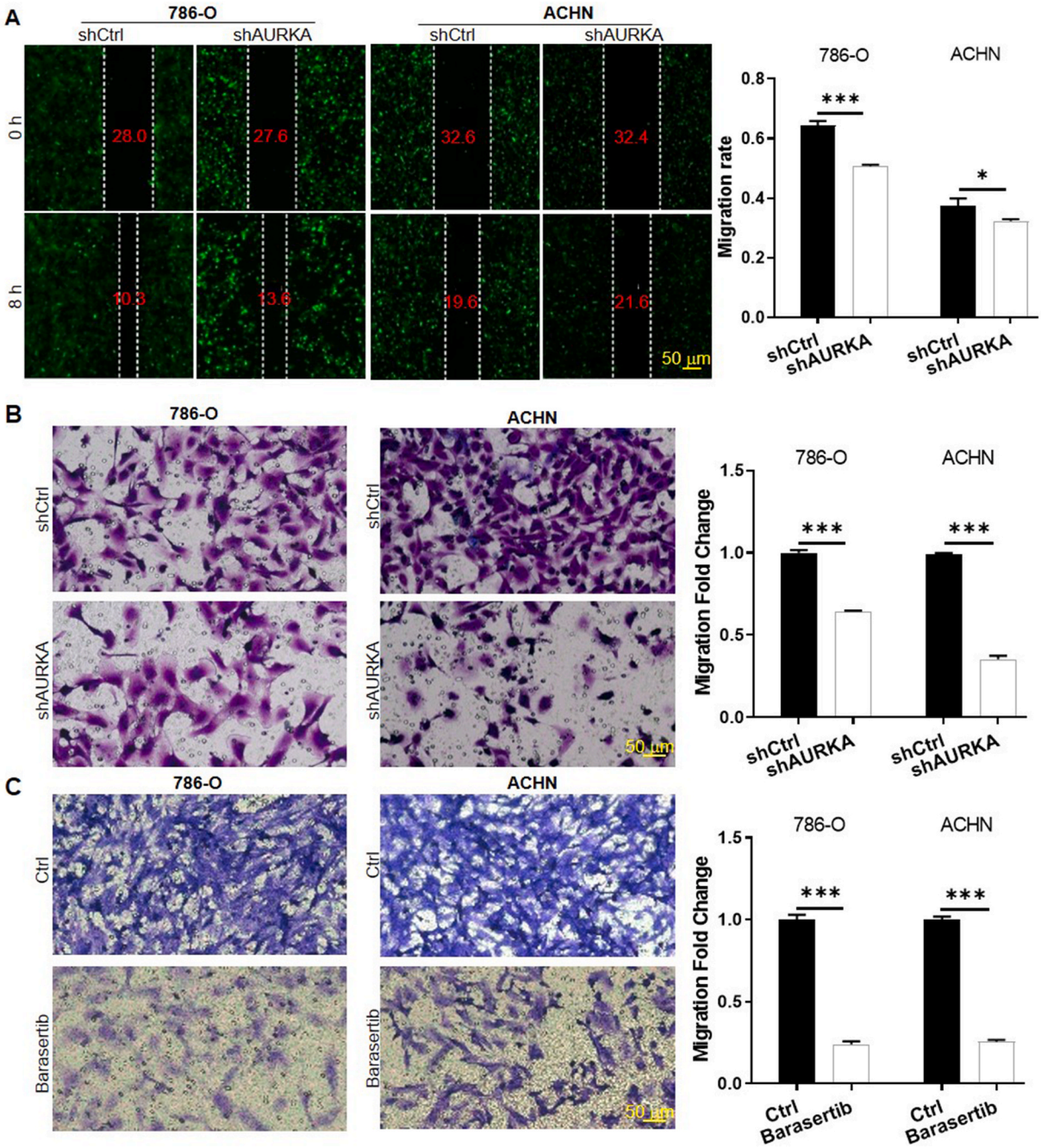

Fig. 3. AURKA inhibition impaired the migratory capacity of RCC cells. (A) Wound-healing assay and (B) Transwell assay were performed to detect the impact of AURKA deficiency on cell migration ability. n = 3. (C) The impact of Barasertib on cell migration was evaluated by transwell assay. Scale bar represents 50 μm. n = 3. $^{*}P < 0.05$, $^{***}P < 0.001$.

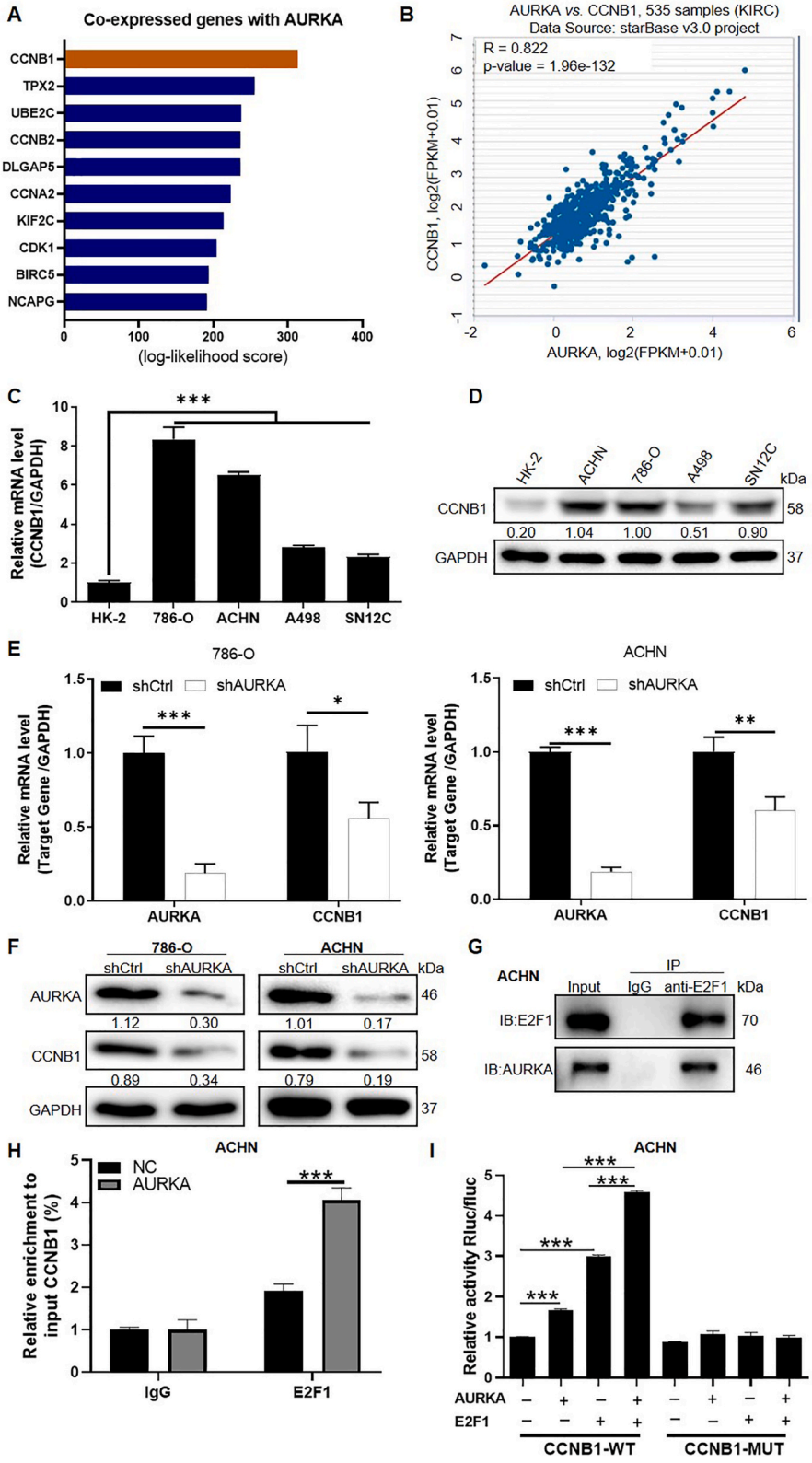

(caption on next page)

Fig. 4. Overexpressed AURKA in ACHN cells regulates CCNB1 transcription. (A) The top 10 of co-expressed genes with AURKA were identified using Coexpedia. The higher likelihood scores (LLS) represent the greater possibility of co-expression. (B) The co-expression correlation analysis between AURKA and CCNB1 in KIRC was performed using ENCORI (https://rna.sysu.edu.cn/encori/panGeneCoExp.php). (C) Relative mRNA and (D) protein levels of CCNB1 in human normal cell line (HK-2) and RCC cell lines (ACHN, 786-O, A498, SN12C). n = 3. (E) Relative mRNA and (F) protein levels of AURKA and CCNB1 were detected in 786-O and ACHN cells with AURKA knockdown. GAPDH served as an inner control. n = 3. (G) Endogenous interaction between AURKA and E2F1 in ACHN cells was confirmed by Co-IP assays. n = 3. (H) ChIP assay indicated the binding of E2F1 and CCNB1 promotor. Chromatins were isolated from AURKA-overexpressed ACHN cells or control ACHN cells. n = 3. (I) Dual-luciferase assay in ACHN cells showed the effect of AURKA and E2F1 expression on CCNB1 promoter activity. n = 3. $^{*}P < 0.05$, $^{**}P < 0.01$, $^{***}P < 0.001$.

the mRNA and protein level of CCNB1, suggesting that AURKA may regulate CCNB1 expression at the transcriptional level (Fig. 4E-F). Therefore, we further predicted the transcription factor E2F1 that regulates CCNB1 online through the TRRUST website (http://www.grnpedia.org/trrust/), implying that AURKA may regulate CCNB1 expression at a transcriptional level through E2F1. In an attempt to confirm the mechanism by which AURKA is recruited to the CCNB1 promoter, we firstly performed the Co-IP experiment. The data revealed that AURKA was co-precipitated with E2F1 in ACHN cells when endogenous E2F1 was pulled down by E2F1 antibody (Fig. 4G). Furthermore, ChIP experiment verified that AURKA could promote the binding of transcription factor E2F1 to the promoter region of CCNB1 (Fig. 4H). We also constructed luciferase plasmids of mutant-type (CCNB1-MUT) and wild-type CCNB1 (CCNB1-WT) promoter regions and co-transfected with E2F1-overexpressed plasmids into AURKA-overexpressed or control ACHN cells. As shown in Fig. 4I, E2F1 overexpression dramatically increased luciferase activity driven by the CCNB1-WT but not the CCNB1-MUT promoter, suggesting a positive regulation of E2F1 on CCNB1. Collectively, our findings supported that overexpression of AURKA in ACHN cells promoted CCNB1 transcription via interacting with E2F1.

3.4. CCNB1 is required for AURKA-mediated proliferation and migration of RCC cells

To determine the synergistic function of AURKA and CCNB1 in RCC cell proliferation and migration, we knocked down CCNB1 expression (shCCNB1-1) in AURKA-overexpressed 786-O and ACHN cells, and performed the *in vitro* and *in vivo* rescue experiments. As shown in Fig. 5A, CCNB1 depletion was able to attenuate the suppression of AURKA on cell apoptosis. Furthermore, a compromised migratory capacity was evident in cells with concurrent overexpression of AURKA and knockdown of CCNB1, in comparison to cells solely overexpressing AURKA (Fig. 5B). In order to further verify the essential role of CCNB1 in AURKA-induced RCC development, animal experiments were carried out accordingly. The tumor growth curve indicated that AURKA accelerated the tumor growth of ACHN cells, which could be reduced by knocking down CCNB1 (Supplementary F. 2A). The results of tumor weight was in accordance with tumor volume (Supplementary F. 2B–2C). The expression of AURKA and CCNB1 in tumor tissues was detected by qPCR (Supplementary F. 2D) and Western blot (Supplementary F. 2E). After the overexpression of AURKA, the expression levels of both AURKA and CCNB1 in tumor tissues exhibited an increase, while the downregulation of CCNB1 had no effect on AURKA expression. In addition, the expression of Ki-67 in the tumor tissue of each group of mice was detected by IHC. The results showed that CCNB1 deficiency also apparently reduced the Ki-67 expression in AURKA-overexpressed tumor tissues (Supplementary F. 2F), indicating that AURKA promoted *in vivo* proliferation of ACHN cells via CCNB1. Taken together, the above results suggested that CCNB1 served as an essential downstream factor of AURKA contributing to RCC progression.

4. Discussion

In view of the pivotal role of AURKA in cell proliferation, its regulatory influence on tumor progression has garnered considerable attention from researchers in recent years. For example, a recent work showed that AURKA promotes m6A modification and stabilization of DROSHA mRNA by preventing ubiquitination and protein degradation of METTL14, ultimately contributing to transcriptional activation of STC1 and functional maintenance of breast cancer stem-like cells [20]. Based on the understanding of the regulatory function of AURKA in tumors, it has emerged as a promising target for anticancer drug development, leading to the creation of numerous small molecule inhibitors for thorough investigation [21–23]. Specifically, CDK4/6 inhibitors have demonstrated the ability to arrest tumor cell mitosis in G1 phase, thereby inhibiting tumor cell proliferation and influencing the treatment outcomes for $HR^{+}/HER2^{-}$ breast cancer patients. Researchers have identified RB1 deletion mutations as a key factor triggering resistance to CDK4/6 inhibitors. The application of the AURKA inhibitor LY3295668 has shown a 'synthetic lethal' effect in breast cancer patients with RB1 deletion mutations, effectively addressing the issue of CDK4/6 inhibitor resistance [21–23]. In addition, the activation of AURKA has been linked to acquired resistance to EGFR-TKI therapy. Alleviating the effect of AURKA can restore sensitivity in resistant tumor cells to EGFR-TKIs. As a result, there is anticipation that combining EGFR-TKIs with AURKA inhibitors could enhance the efficacy of first-line therapy [22,24]. Therefore, the current study aims to reveal the role of AURKA in promoting RCC progression. The findings seek to provide a theoretical foundation for the development of targeted agents against AURKA, offering potential avenues for therapeutic interventions in RCC.

AURKA has consistently demonstrated its oncogenic role in promoting tumorigenesis across various cancer types, including RCC [25]. Analysis of TCGA data revealed high expression levels of AURKA in adrenocortical carcinoma (ACC), KICH, KIRC and KIRP [26]. Beyond RCC, AURKA overexpression has been observed in diverse tumor types such as lung adenocarcinoma (LUAD), liver hepatocellular carcinoma (LIHC), uveal melanoma (UVM), mesothelioma (MESO), breast cancer and pancreatic carcinoma [20,26–28]. Consistent with these findings, our study confirmed the upregulation of AURKA expression in RCC tissues and cell lines. Moreover, overexpression of AURKA were associated with advanced TNM level and pathological stage, as well as a poor survival rates. AURKA's

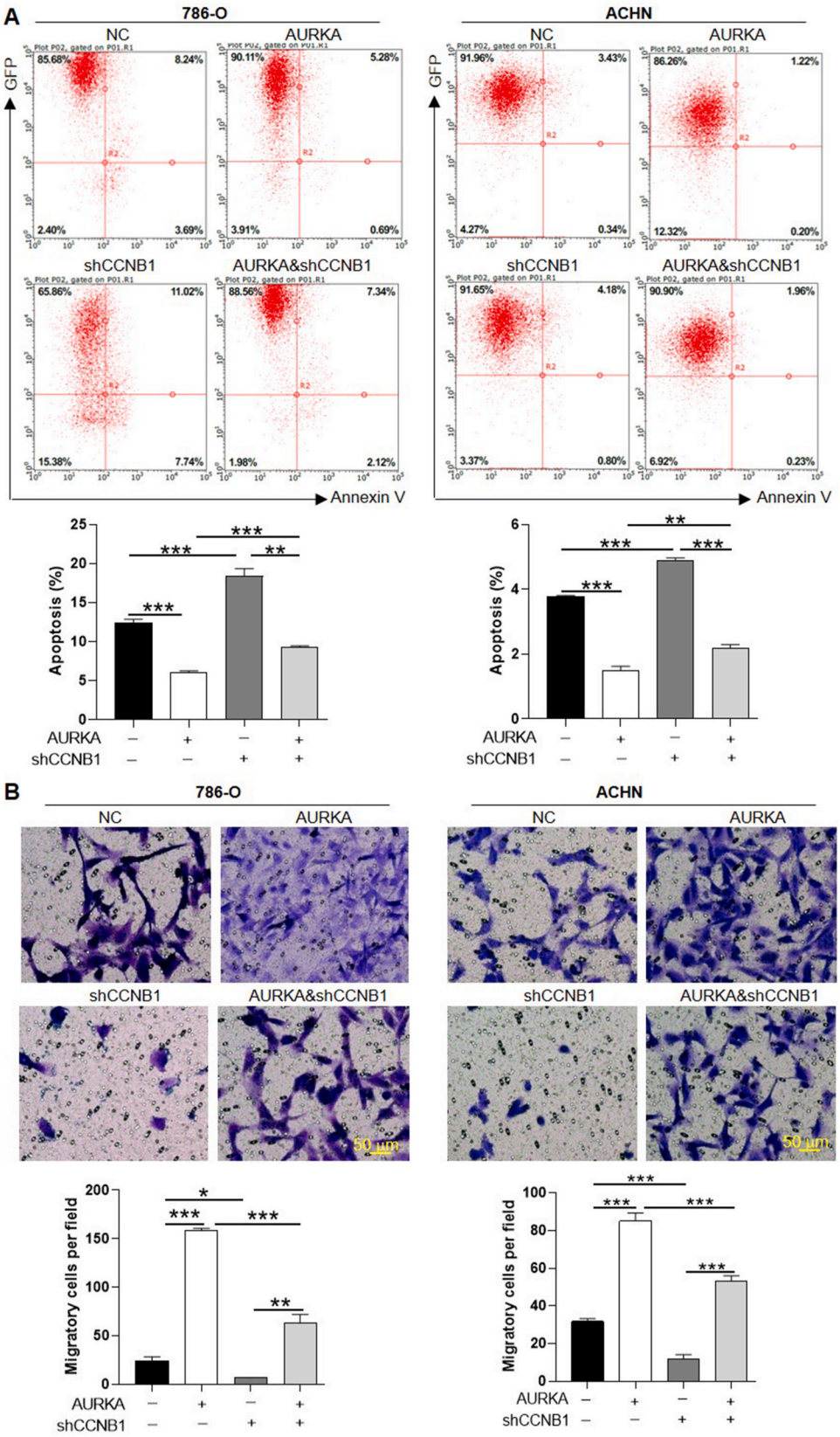

(caption on next page)

Fig. 5. CCNB1 is required for AURKA-mediated proliferation and migration of RCC cells *in vitro*. (A) 786-O and ACHN cells were infected with indicated lentiviruses, the significance of CCNB1 on AURKA-induced anti-apoptosis was assessed by flow cytometry. n = 3. (B) The transwell assays were then performed for evaluating the essential role of CCNB1 in AURKA-mediated cell migration. Scale bar is 50 μm. n = 3. $^{*}P < 0.05$, $^{**}P < 0.01$, $^{***}P < 0.001$.

role as a tumor promoter is further supported by evidence showing that its inhibition by the specific inhibitor CCT137690 slowed the growth of pancreatic ductal adenocarcinoma cancer (PDAC) cells in murine models [27]. Moreover, Wang et al. reported AURKA's involvement in the development of non-small cell lung cancer (NSCLC) by affecting autophagy and radiosensitivity of NSCLC cells [29]. Additionally, nuclear AURKA was found to increase PD-L1 expression via a myc-dependent pathway, leading to immunosuppression and tumor progression [30]. To demonstrate the promoting role of AURKA in RCC, we employed AURKA shRNA and its inhibitor Barasertib to downregulate AURKA and explored their effect on malignant phenotypes. Our results demonstrated that both AURKA shRNA-mediated knockdown and Barasertib-induced inhibition significantly impaired the proliferative and migratory abilities of RCC cells, and induced cell apoptosis. Moreover, AURKA knockdown arrested the cell cycle at G1/G2 phase, and decrease the expression of cell cycle regulators, including CCNB1, CCND1 and CCNA1. These findings collectively affirm the tumorigenic role of AURKA in RCC.

We further revealed that CCNB1 serve as a potential target gene of AURKA, and AURKA regulated CCNB1 transcription through the transcription factor E2F1. E2F1 is a well-characterized regulator involved in critical cellular processes such as the cell cycle, cell proliferation, apoptosis and DNA damage repair [31,32]. Functioning by directly binding to the DNA sequence of genes, E2F1 regulates the transcriptional activity of downstream genes, including CCNB1 [33]. CCNB1, a regulatory protein in the cell cycle, plays an important role in the process of cell division and mitosis [34]. Pan et al. reported the upregulation of Cyclin B1 (CCNB1) signaling in RCC, mediating RCC tumorigenesis induced by EIF3D [35]. In line with this, our study revealed the overexpression of CCNB1 in RCC, correlating positively with poor prognosis. Further studies suggested that AURKA physically interacts with E2F1 and subsequently forms a complex with E2F1 on the promoter region of CCNB1. CCNB1 deficiency led to an inhibition of proliferation and migration induced by AURKA in RCC cells. Therefore, the regulatory axis of AURKA influencing CCNB1 is sufficient to control RCC development.

In conclusion, our findings open up intriguing possibilities, suggesting that AURKA might be a novel target for RCC therapeutics. Moreover, the crucial role of CCNB1 signaling in the malignant characteristics of RCC cells implies that targeting CCNB1 expression by suppressing AURKA may serve as an alternative therapeutic strategy for treating RCC. However, there were no biological replicates in animal experiments, and the sample size for each experimental group was relatively small, which is a limitation of our study. Therefore, a larger number of animal samples and more rigorous scientific methodologies are required in the future to substantiate our findings.

Funding

This research was supported by the Top-level Clinical Discipline Project of Shanghai Pudong (PWYgf2021-07).

Ethics approval and consent to participate

The Ethical Committee of Shanghai East Hospital, Tongji University approved the usage of human tissues and animal experimentation in this study (approval no. 2020-128). Informed consents were obtained from the patients involved. For the animal study, adherence to the ARRIVE guidelines (https://arriveguidelines.org) was ensured, and every effort was made to minimize animal suffering. In summary, all methods and procedures conducted in this study strictly adhered to relevant regulations and guidelines.

Data availability statement

The data set supporting the results of this article are included within the article.

CRediT authorship contribution statement

Jiling Wen: Writing – review & editing, Writing – original draft, Validation, Supervision, Project administration, Investigation, Data curation, Conceptualization. **Xuechun Wang:** Writing – original draft, Supervision, Software, Resources, Investigation, Formal analysis. **Guosheng Yang:** Writing – original draft, Software, Resources, Methodology, Investigation, Formal analysis, Data curation. **Junhua Zheng:** Writing – review & editing, Writing – original draft, Visualization, Validation, Conceptualization.

Declaration of competing interest

The authors declare that they have no known competing financial interests or personal relationships that could have appeared to influence the work reported in this paper.

Acknowledgements

None.

Appendix A. Supplementary data

Supplementary data to this article can be found online at https://doi.org/10.1016/j.heliyon.2024.e27959.

References

[1] R.L. Siegel, K.D. Miller, H.E. Fuchs, et al., Cancer statistics, 2022, Ca - Cancer J. Clin. 72 (1) (2022) 7–33, https://doi.org/10.3322/caac.21708.
[2] H. Sung, J. Ferlay, R.L. Siegel, et al., Global cancer statistics 2020: GLOBOCAN estimates of incidence and mortality worldwide for 36 cancers in 185 countries, Ca - Cancer J. Clin. 71 (3) (2021) 209–249, https://doi.org/10.3322/caac.21660.
[3] D. Singh, Current updates and future perspectives on the management of renal cell carcinoma, Life Sci. 264 (2021) 118632, https://doi.org/10.1016/j.lfs.2020.118632.
[4] S.R. Williamson, Clear cell papillary renal cell carcinoma: an update after 15 years, Pathology 53 (1) (2021) 109–119, https://doi.org/10.1016/j.pathol.2020.10.002.
[5] N. Chowdhury, C.G. Drake, Kidney cancer: an overview of current therapeutic approaches, Urol. Clin. 47 (4) (2020) 419–431, https://doi.org/10.1016/j.ucl.2020.07.009.
[6] M. Garg, D. Kanojia, A. Khosla, et al., Sperm-associated antigen 9 is associated with tumor growth, migration, and invasion in renal cell carcinoma, Cancer Res. 68 (20) (2008) 8240–8248, https://doi.org/10.1158/0008-5472.CAN-08-1708.
[7] E.M. Posadas, S. Limvorasak, R.A. Figlin, Targeted therapies for renal cell carcinoma, Nat. Rev. Nephrol. 13 (8) (2017) 496–511, https://doi.org/10.1038/nrneph.2017.82.
[8] Y. Lai, F. Tang, Y. Huang, et al., The tumour microenvironment and metabolism in renal cell carcinoma targeted or immune therapy, J. Cell. Physiol. 236 (3) (2021) 1616–1627, https://doi.org/10.1002/jcp.29969.
[9] C. Dominguez-Brauer, K.L. Thu, J.M. Mason, et al., Targeting mitosis in cancer: emerging strategies, Mol Cell 60 (4) (2015) 524–536, https://doi.org/10.1016/j.molcel.2015.11.006.
[10] A.S. Nikonova, I. Astsaturov, I.G. Serebriiskii, et al., Aurora A kinase (AURKA) in normal and pathological cell division, Cell. Mol. Life Sci. 70 (4) (2013) 661–687, https://doi.org/10.1007/s00018-012-1073-7.
[11] I.A. Asteriti, F. De Mattia, G. Guarguaglini, Cross-talk between AURKA and Plk1 in mitotic entry and spindle assembly, Front. Oncol. 5 (2015) 283, https://doi.org/10.3389/fonc.2015.00283.
[12] J. Tischer, F. Gergely, Anti-mitotic therapies in cancer, J. Cell Biol. 218 (1) (2019) 10–11, https://doi.org/10.1083/jcb.201808077.
[13] F. Wang, H. Zhang, H. Wang, et al., Combination of AURKA inhibitor and HSP90 inhibitor to treat breast cancer with AURKA overexpression and TP53 mutations, Med. Oncol. 39 (12) (2022) 180, https://doi.org/10.1007/s12032-022-01777-x.
[14] K. Sasai, W. Treekitkarnmongkol, K. Kai, et al., Functional significance of aurora kinases-p53 protein family interactions in cancer, Front. Oncol. 6 (2016) 247, https://doi.org/10.3389/fonc.2016.00247.
[15] Y. Wang, Z. Wang, Z. Qi, et al., The negative interplay between Aurora A/B and BRCA1/2 controls cancer cell growth and tumorigenesis via distinct regulation of cell cycle progression, cytokinesis, and tetraploidy, Mol. Cancer 13 (2014) 94, https://doi.org/10.1186/1476-4598-13-94.
[16] O. Haonon, R. Rucksaken, P. Pinlaor, et al., Upregulation of 14-3-3 eta in chronic liver fluke infection is a potential diagnostic marker of cholangiocarcinoma, Proteonomics Clin. Appl. 10 (3) (2016) 248–256, https://doi.org/10.1002/prca.201500019.
[17] K.J. Livak, T.D. Schmittgen, Analysis of relative gene expression data using real-time quantitative PCR and the 2(-Delta Delta C(T)) Method, Methods 25 (4) (2001) 402–408, https://doi.org/10.1006/meth.2001.1262.
[18] L. Yang, M. Jin, S.J. Park, et al., SETD1A promotes proliferation of castration-resistant prostate cancer cells via FOXM1 transcription, Cancers 12 (7) (2020), https://doi.org/10.3390/cancers12071736.
[19] B. Chen, J. Lai, D. Dai, et al., PARPBP is a prognostic marker and confers anthracycline resistance to breast cancer, Ther Adv Med Oncol 12 (2020) 1758835920974212, https://doi.org/10.1177/1758835920974212.
[20] F. Peng, J. Xu, B. Cui, et al., Oncogenic AURKA-enhanced N(6)-methyladenosine modification increases DROSHA mRNA stability to transactivate STC1 in breast cancer stem-like cells, Cell Res. 31 (3) (2021) 345–361, https://doi.org/10.1038/s41422-020-00397-2.
[21] K.N. Shah, R. Bhatt, J. Rotow, et al., Aurora kinase A drives the evolution of resistance to third-generation EGFR inhibitors in lung cancer, Nat. Med. 25 (1) (2019) 111–118, https://doi.org/10.1038/s41591-018-0264-7.
[22] C.Y. Wang, M.H. Lee, Y.R. Kao, et al., Alisertib inhibits migration and invasion of EGFR-TKI resistant cells by partially reversing the epithelial-mesenchymal transition, Biochim. Biophys. Acta Mol. Cell Res. 1868 (6) (2021) 119016, https://doi.org/10.1016/j.bbamcr.2021.119016.
[23] J. Wang, T. Hu, Q. Wang, et al., Repression of the AURKA-CXCL5 axis induces autophagic cell death and promotes radiosensitivity in non-small-cell lung cancer, Cancer Lett. 509 (2021) 89–104, https://doi.org/10.1016/j.canlet.2021.03.028.
[24] J. Chen, H. Lu, W. Zhou, et al., AURKA upregulation plays a role in fibroblast-reduced gefitinib sensitivity in the NSCLC cell line HCC827, Oncol. Rep. 33 (4) (2015) 1860–1866, https://doi.org/10.3892/or.2015.3764.
[25] X. Gong, J. Du, S.H. Parsons, et al., Aurora A kinase inhibition is synthetic lethal with loss of the RB1 tumor suppressor gene, Cancer Discov. 9 (2) (2019) 248–263, https://doi.org/10.1158/2159-8290.CD-18-0469.
[26] R. Du, C. Huang, K. Liu, et al., Targeting AURKA in Cancer: molecular mechanisms and opportunities for Cancer therapy, Mol. Cancer 20 (1) (2021) 15, https://doi.org/10.1186/s12943-020-01305-3.
[27] Y. Xie, S. Zhu, M. Zhong, et al., Inhibition of aurora kinase A induces necroptosis in pancreatic carcinoma, Gastroenterology 153 (5) (2017) 1429–1443 e1425, https://doi.org/10.1053/j.gastro.2017.07.036.
[28] S.Y. Hong, Y.C. Lu, S.H. Hsiao, et al., Stabilization of AURKA by the E3 ubiquitin ligase CBLC in lung adenocarcinoma, Oncogene 41 (13) (2022) 1907–1917, https://doi.org/10.1038/s41388-022-02180-6.
[29] A. Almilaibary, Targeting aurora kinase a (AURKA) in cancer: molecular docking and dynamic simulations of potential AURKA inhibitors, Med. Oncol. 39 (12) (2022) 246, https://doi.org/10.1007/s12032-022-01852-3.
[30] S. Sun, W. Zhou, X. Li, et al., Nuclear Aurora kinase A triggers programmed death-ligand 1-mediated immune suppression by activating MYC transcription in triple-negative breast cancer, Cancer Commun. 41 (9) (2021) 851–866, https://doi.org/10.1002/cac2.12190.
[31] S. Fouad, D. Hauton, V. D'Angiolella, E2F1: cause and consequence of DNA replication stress, Front. Mol. Biosci. 7 (2020) 599332, https://doi.org/10.3389/fmolb.2020.599332.
[32] M.G. Ertosun, F.Z. Hapil, O. Osman Nidai, E2F1 transcription factor and its impact on growth factor and cytokine signaling, Cytokine Growth Factor Rev. 31 (2016) 17–25, https://doi.org/10.1016/j.cytogfr.2016.02.001.

[33] W. Bertrams, K. Griss, M. Han, et al., Transcriptional analysis identifies potential biomarkers and molecular regulators in acute malaria infection, Life Sci. 270 (2021) 119158, https://doi.org/10.1016/j.lfs.2021.119158.
[34] B. Xie, S. Wang, N. Jiang, et al., Cyclin B1/CDK1-regulated mitochondrial bioenergetics in cell cycle progression and tumor resistance, Cancer Lett. 443 (2019) 56–66, https://doi.org/10.1016/j.canlet.2018.11.019.
[35] X.W. Pan, L. Chen, Y. Hong, et al., EIF3D silencing suppresses renal cell carcinoma tumorigenesis via inducing G2/M arrest through downregulation of Cyclin B1/CDK1 signaling, Int. J. Oncol. 48 (6) (2016) 2580–2590, https://doi.org/10.3892/ijo.2016.3459.